RSC Advances




ROYAL SOCIETY OF CHEMISTRY

www.rsc.org/advances

# Magnetic anisotropic properties of Pd/Co/Pd trilayer films studied by x-ray absorption spectroscopy and magnetic circular dichroism

K. Saravanan,[a] C.-H. Kao,[a] Y.-C. Shao,[a] Y.-F. Wang,[a] B.-Y. Wang,[b,*] H. T. Wang,[c] C.-J. Tsai,[d] W.-C. Lin,[d] C.-W. Pao,[e] H.-M. Tsai,[e] L.-Y. Jang,[e] H. J. Lin,[e] J.-F. Lee[e] and W.-F. Pong[a,*]

[a] *Department of Physics, Tamkang University, Tamsui 251, Taiwan*

[b] *Department of Physics, National Changhua University of Education, Changhua 500, Taiwan*

[c] *Department of Physics, National Tsinghua University, Hsinchu 300, Taiwan*

[d] *Department of Physics, National Taiwan Normal University, 116 Taipei, Taiwan*

[e] *National Synchrotron Radiation Research Center, Hsinchu 300, Taiwan*

## Abstract

We study the magnetic anisotropic properties of as-grown and annealed Pd/Co/Pd trilayer films based on their atomic and electronic structures using extended x-ray absorption fine structure (EXAFS), x-ray absorption near edge structure (XANES) spectroscopy and magnetic circular dichroism (XMCD) measurements. The annealed film exhibits interesting perpendicular magnetic anisotropy (PMA) whereas as-grown film exhibits in-plane anisotropy. Cross-sectional transmission electron microscopic analysis together with the Co *K*-edge EXAF results confirm the formation of ordered-alloy CoPd phase in the annealed film, whereas the as-grown film has *hcp* Co-like phase. Co $L_{3,2}$-edge XMCD measurements reveal an enhanced ratio of Co 3*d* orbital to spin moments of the annealed film providing evidence of the observed PMA upon annealing.

*Corresponding authors: bywang1735@gmail.com & wfpong@mail.tku.edu.tw

## INTRODUCTION

Magnetic thin films with perpendicular magnetic anisotropy (PMA) have great research interest due to their applications in featured high-density non-volatile memory and magnetic memory devices with the possibility of current-induced magnetization switching.[1,2] In these films, it is able to facilitate faster and smaller data-storage magnetic bits, compared with the normal in-plane ones.[3] In a magnetic material, the spin-orbit interaction of the electrons plays a major role in determining the anisotropy behavior.[4] To attain perpendicular anisotropy, a number of material systems have been explored by various research groups and these materials include rare-earth/transition-metal alloys, $L1_0$-ordered (Co, Fe)–Pt alloys and Co/(Pd, Pt) multilayers.[2-7] In such alloys, the electronic hybridization of valence levels of 3*d* transition metal, with large magnetic moments but relatively small spin–orbit coupling (Fe or Co), with valence levels of 4*d*, 5*d* transition metals (Pd or Pt) with small magnetic moments but a large spin–orbit coupling, alters the spin-orbit interaction which could enhance the PMA.[8,9] Among the alloys, the Co/Pd composites exhibit attractive magnetic properties and have been studied extensively by many research groups.[10-13]

Yakushiji *et al.* have observed an enhanced PMA with a large anisotropy energy in $[Co/Pt]_n$ and $[Co/Pd]_n$ superlattice films consisting of 0.14-0.20 nm thick Co and Pt(Pd) layers.[14] These $[Co/Pt(or\ Pd)]_n$ superlattice films had a post-annealing stability of up to 370°C due to the formation of the ordered-alloy-like structure, in which the inter-diffusion of Co and Pt(Pd) atoms was suppressed. Carrey *et al.* have studied the perpendicular anisotropy in Co/Pd multilayers with the structure: $[(\sim 0.3$ nm Co co-deposited with $y$ nm Pd)/$(2.0-y)$ nm $Pd]_{15}$ , with $y$ = 0, 0.1, 0.3, 0.5, 1, 1.5 and 2.0.[13]

The perpendicular anisotropy is almost unaffected by alloying up to $y$= 0.5 nm. With further increase of $y$, the magnetic coercivity, saturation field and squareness are decreased exponentially. Most of Co/Pd multilayers exhibit PMA when the Co thickness is very less. Specifically, Co film of thickness ~0.8 nm is highly suggested for enhanced perpendicular magnetization.[15,16] This is mainly due to tensile strain at the interface due to the lattice mismatch with the Pd layer. On the other hand, The Pd layer thickness also plays a significant role in tuning the spin orientation in the CoPd composites.[16-18] Kim *et al*. have studied the magnetization property of Pd(50Å)/CoPd(20Å)/Pd($t_{Pd}$) film as a function of Pd layer thickness ($t_{Pd}$).[18] These authors observed that the magnetization direction smoothly changes from in-plane orientation (at $t_{Pd}$ = 0 Å) through canted out of plane (0< $t_{Pd}$ < 30 Å) to perpendicular (30 < $t_{Pd}$ < 60 Å). From these results, it is clear that a well controlled thickness of Co, Pd films and multilayered structures are essential to achieve the desired PMA in CoPd composites. Yabuhara *et al*. have also observed that in-plane anisotropy in CoPd films prepared by rf magnetron sputtering.[20] These authors concluded that the in-plane magnetic anisotropy of CoPd films is due to disordered CoPd alloy crystal. Hence, a detailed analysis is necessary to clarify the correlation between the structure and magnetic anisotropy in this alloy system. Many research groups have observed that high-temperature annealing enhanced PMA,[9,21] however, the effect of temperature on alloy formation, particularly the relationships among the atomic and electronic structures, magnetic moments and PMA of magnetic ion such as Co are not fully understood. To solve these problems, a simple method for synthesizing CoPd alloy with better understanding of factors that enhancing the PMA is necessary.

The present work explores a simple method to synthesis CoPd alloy nanostructure,

which shows strong PMA behavior, by in-situ annealing of Pd(4nm)/Co(5nm)/Pd(4nm) trilayer film. The film thicknesses are considerable large in comparison with the earlier reports.[13-17,22] It is observed that the high temperature annealing rigorously alters the arrangement of atoms in the layer structure. As the spin-orbit interaction plays a major role in PMA, the quantification of spin, orbital moments and electronic and atomic structural properties are essential for better understanding of anisotropy behavior of a material. We have studied the atomic and electronic structural properties of the as-grown and annealed films using synchrotron radiation based X-ray absorption measurements, which are highly proven techniques to study the local atomic, electronic structure and magnetic properties of a material.[8,23] The observed PMA behavior of annealed film has been discussed in detail with the help of these sensitive techniques.

## EXPERIMENTAL DETAILS

Investigation of the Pd/Co/Pd films was performed at room temperature at National Synchrotron Radiation Research Center (NSRRC) in Hsinchu, Taiwan. The electronic structure of the Pd/Co/Pd films was measured by Pd $L_{3,2}$-edge X-ray absorption near-edge structure (XANES) at beamline BL-16A in total fluorescence yield (TFY) mode with an angle of 45° between the incident X-rays and the surface normal. The local atomic structure of the Co atoms in the films were measured by extended X-ray absorption fine structure (EXAFS) at beamline BL-17C. For probing the magnetic properties of samples, Co $L_{3,2}$-edge XANES and X-ray magnetic circular dichroism (XMCD) were performed at beamline BL-11A at NSRRC as well. The spectra were recorded in total electron yield (TEY) mode. For the XMCD measurement, the incident angle of X-rays was fixed at 30°

from the sample normal, and a magnetic field of 1 Tesla was applied parallel and antiparallel to the sample normal.

The Pd/Co/Pd thin trilayers were deposited on $Al_2O_3$ (0001) substrate by similar molecular beam epitaxy (MBE) method under ultra high vacuum condition with a base pressure better than $3\times10^{-9}$ torr. The deposition rate was maintained ~1 nm/min for uniform deposition of films. With identical condition, two Pd(4nm)/Co(5nm)/Pd(4nm) samples were prepared at room temperature. After deposition, one of them was *in-situ* annealed at 700 K for 250 seconds. In order to understand the mechanism of the PMA behavior, Pd-rich (approximately $Pd_{75}Co_{25}$) and Co-rich (approximately $Pd_{25}Co_{75}$) alloys were also prepared by similar MBE using co-evaporation from individual Co and Pd targets with controlled rate of deposition to achieve the desired composition. The cross-sectional view of the deposited films were analyzed using transmission electron microscopy (TEM) equipped with energy dispersive spectroscopy (EDS) facility. Please note that the spatial resolution of TEM-EDS was determined by both size of the incident *e*-beam and its relative spreading in the sample. In our TEM measurement, the *e*-beam size is ~1 nm and its spreading in the sample is in few nm. Therefore, we can conclude that the spatial resolution of TEM-EDS analysis is within few nanometers scale. The magnetic properties of all the films were *ex-situ* investigated using magneto-optical Kerr effect (MOKE). The MOKE measurement system was composed of four electromagnet poles installed in a vacuum chamber, so that the MOKE hysteresis loops were measured in both perpendicular and in-plane geometries by simply switching the polarity of electromagnet without changing the optical setup.[11]

## RESULTS AND DISCUSSION

Figures 1 (a) and 1(b) show the in-plane and out-of-plane MOKE magnetic hysteresis loops of as-grown and annealed Pd/Co/Pd films, respectively. The insets show the corresponding cross-sectional TEM images and EDS scan across the film interface. It is clear that in as-grown film the Co and Pd films have individual layer structures, whereas in annealed film they are mixed with each other. The elemental line profile based on the EDS scan across the film also confirms a mixing of the Co and Pd layers upon annealing. This is in contrast with earlier reports of ultrathin Co/Pd multilayers where the inter-diffusion was suppressed.[14] The as-grown Pd/Co/Pd film exhibits in-plane magnetization [Fig. 1(a)], whereas annealed film exhibits a strong PMA with a weak in-plane magnetization [Fig. 1(b)]. Generally in a magnetic thin film, the magnetic dipolar interaction causes shape anisotropy where the magnetization lies within the plane of the film, while the spin-orbit interaction in certain crystalline structures could cause magnetocrystalline anisotropy which is perpendicular to the plane.[23,24] The effective anisotropy is the resultant of these two competitive interactions in a magnetic thin film. In the present work, the in-plane anisotropy observed in as-grown film could be simply attributed to the dominated shape anisotropy owing to a thick layer of Co film (~5 nm).[4] In case of annealed film, the Pd layers have strong effect on the magnetization orientation. This result may be correlated with a formation of CoPd alloy upon annealing. To further elucidate the correlation between the magnetic anisotropy and alloy structure, MOKE measurements have also been performed on Pd-rich and Co-rich alloy films and are shown in Figs. 1(c) and 1(d), respectively. The inset shows the corresponding cross-sectional TEM images and the EDS analysis. The thickness of Pd-rich alloy (~16.1

nm) is close to the annealed film (~14.4 nm), whereas the thickness of Co-rich alloy is large (~38.3 nm). The MOKE measurements reveal that the Co-rich alloy has in-plane magnetization while the Pd-rich alloy has in-plane as well as perpendicular magnetizations. Furthermore, the PMA of annealed film was also found to differ from the disordered CoPd alloy which exhibits in-plane anisotropy.[20] These findings suggest that the magnetic anisotropy of CoPd film is highly sensitive to the alloy composition and structural orderings.

In order to observe the local atomic structure of the synthesized films, EXAFS measurements have been carried out at Co *K*-edge. Figure 2(a) represents the Fourier transform (FT) spectra of the Co *K*-edge EXAFS of as-grown and annealed Pd/Co/Pd films along with the references. The inset shows the corresponding EXAFS $k^2\chi$ data. For the as-grown film, the spectral features and the main feature ~2.1 Å (without phase correction), which is correspond to the nearest-neighbor (NN) Co-Co bond distance, are same as reference Co foil, indicating no random mixing between Co and Pd.[25] However, the peak intensity is slightly reduced because of slight disorder in the film due to thickness effect. In contrast to the as-grown film, the annealed film exhibits two main FT features in the region ~1.6-3.0 Å, which corresponds to NN Co-Co and Co-Pd bond distances and are characteristic of the Co-Pd alloy phase.[12,17,18,22] In Fig. 2(a), it is noticed that the spectral feature of the annealed film is relatively close to the Pd-rich alloy than the Co-rich alloy films. Such a finding can be explained by the uniform mixing of Co atoms in the surrounding Pd atoms, as evidenced by TEM-EDS analysis. By comparing the intensity of the EXAFS features, it is inferred that in annealed film, the NN Co-Co bond is more in comparison with Pd-rich alloy while the Co-Pd bond is slightly lower

than in Pd-rich alloy. The TEM-EDS and EXAFS analyses reveal that the high temperature annealing results an alloying CoPd phase in Pd/Co/Pd trilayer film.

To find the origin of the magnetism in the synthesized CoPd composites, electronic structural studies have been performed using XANES at Pd $L_{3,2}$-edge and the normalized spectra are shown in Fig. 2(b). All XANES spectra exhibit a broad white line (WL) feature A at ~3174 eV, which is attributed primarily to electron transitions from Pd 2*p* orbitals to unoccupied 4*d* conduction band states. High intensity and a slight energy shift of the WL feature of the studied samples relative that to the reference Pd foil are observed. The inset in Fig. 2(b) shows the magnified region of feature A, and reveals that the as-grown film and Pd-rich alloy have similar WL features, whereas the annealed film and Co-rich alloy have blue shifted WL features. According to literature,[26] this blue-shift of the WL feature is associated with charge transfer from Co to Pd atoms, which is caused by strong hybridization of Pd 4*d* and Co 3*d* orbitals and the different electro-negativities of the atoms.[27] This process causes higher energy of X-ray to be required to excite the electrons from Pd 2*p* orbitals to unoccupied 4*d* states. The transfer of charge from Co to Pd atoms promotes the generation of a magnetic moment in the CoPd alloy and acts as the origin of the magnetism in such alloy system.[28] It should be noted that in Co-rich alloy, the shifted is large, this is because of the Pd atom is surrounded by more Co atoms which can provide more charge to the Pd site.

To understand the anisotropy behavior of the synthesized films, XMCD measurements at Co $L_{3,2}$-edge have been performed. The extracted orbital ($m_{orb}$) and spin ($m_{spin}$) magnetic moments are the essential quantities to understand the anisotropy properties of the present systems. Figure 3 displays the Co $L_{3,2}$-edge XANES spectra of the as-grown

and annealed films along with the reference samples, with the photo-helicity of incident X-rays parallel ($\mu_+$) and anti-parallel ($\mu_-$) to the direction of magnetization. All the films exhibit two broad features in the ranges 777-785 eV and 792-800 eV, which are attributed to Co $2p_{3/2} \rightarrow 3d_{5/2}$ and $2p_{1/2} \rightarrow 3d_{3/2}$ dipole transitions, respectively. Figure 3 also presents Co $L_{3,2}$-edge XMCD spectra (bottom panels), $(\mu_+ - \mu_-)/(\mu_+ + \mu_-)$, in which the general line shapes are consistent with those reported elsewhere.[29] All the XMCD curves, integrated over the respective $L_{3,2}$-edges, are related to the $m_{\mathrm{orb}}$ and $m_{\mathrm{spin}}$ *via* the sum rules,[29-31]

$$m_{orb} = -\frac{4q}{3r} \times (10 - n_{3d}) \qquad (1)$$

and

$$m_{spin} = -\frac{6p - 4q}{r} \times (10 - n_{3d}) \left(1 + \frac{7\langle T_z \rangle}{2\langle S_z \rangle}\right)^{-1} \qquad (2)$$

where $n_{3d}$ is the 3*d* electron occupation number of the specific transition metal atom. *p* and *q* are the integrated values of the XMCD curves correspond to the $L_3$ and $L_2$ transitions, respectively. *r*- is the integrated value of the sum $(\mu_+ + \mu_-)$ from XAS spectra, as shown in Fig. 3. $\langle T_z \rangle$- is the expectation value of the magnetic dipole operator, and $\langle S_z \rangle$ equals half of $m_{spin}$ in Hartree atomic units. Generally, the magnetic dipolar term $\langle T_z \rangle$ is less than 10 % of the value of $S_z$. Thus, the ratio of $m_{\mathrm{orb}}$ and $m_{\mathrm{spin}}$ values can be derived from the XMCD data by neglecting these terms in Eq. (2), and using the value $n_{3d}$ = 7.51 for Co.[29] Similarly, the magnetic moments of the Co foil, Co-rich and Pd-rich alloys were also calculated.

Table 1 summarizes the $m_{\mathrm{orb}}$ and $m_{\mathrm{spin}}$ moments and their ratio of all samples measured

along out-of-plane direction. The estimated $m_{orb}$ and $m_{spin}$ values of the standard Co foil are in agreement with the reported value of *hcp* Co.[29] The estimated values of $m_{orb}$ and $m_{spin}$ of as-grown film are larger than that of reference Co foil. This may due to the strain generated by the lattice mismatch at Pd-Co interfaces.[4,27] Interestingly, the $m_{spin}$ value of Co atoms in all films (except the as grown film) is relatively lower than that of the Co foil. In particular, the value is drastically reduced in Pd-rich alloy. This effect could be attributable to the formation of CoPd alloy. Generally in a magnetic material, the value of magnetic moment is associated with the degree of long-range magnetic order, which is determined by a competition between exchange coupling among electrons and thermal fluctuation. Consequently, the $m_{spin}$ would exhibit a higher value at low temperature owing to a less thermal fluctuation, but decrease rapidly as it close to the Curie temperature ($T_C$). For a bulk Co, the $T_C$ is ~1288 K,[4] and therefore sizeable magnetic moments can be simply obtained at room temperature. As the Co concentration decreases, the exchange interaction among Co atoms in the alloy becomes weaker, and the $T_C$ is reduced significantly from 1288 K to 1200 K for 75% Co alloy to 295 K for 8.9 % Co alloy. For the present Pd-rich alloy film, the $T_C$ is estimated to be ~560 K.[32] Such a low $T_C$ could lead to a weak long-range magnetic ordering of the Co atoms at room temperature. Consequently, the $m_{spin}$ of Co atoms in Pd-rich alloy is drastically reduced compared to the reference Co foil. Following the above discussion, the reduction of $m_{spin}$ and $m_{orb}$ values of annealed film, in comparison with as-grown film, could be attributed to a formation of CoPd alloy. On the other hand, although the atomic structure of annealed film is similar to the Pd-rich alloy, the values of the $m_{orb}$ and $m_{spin}$ are much higher than those of Pd-rich alloy. This can be due to the formation of CoPd alloy with high order

structure of annealed film, which generally posses a higher moment than that of the non-crystallographic morphologies.[33]

According to previous reports, the $m_{orb}/m_{spin}$ ratio measured along out-of-plane direction could roughly be considered as an indication for the presence of the perpendicular $K_{cry}$ in a magnetic film.[34-37] Nevertheless, the presence of PMA is not only determined by the $K_{cry}$ but also the total magnetic moment (i.e. $m_{orb} + m_{spin}$) of the film. This is because, the total magnetic moments would contribute the shape anisotropy ($K_{shape} = -2\pi M^2$, where $M$ is saturation magnetization) which prefers in-plane direction. Thus, only if the magnitude of positive $K_{cry}$ can overcome the negative in-plane shape anisotropy energy, the magnetization of thin film would tend to align out-of-plane direction.[24] In the present work, as shown in Table 1, it is clear that the $m_{orb}/m_{spin}$ ratio of the annealed Pd/Co/Pd film is higher than the as-grown film. This gives clear evidence to the enhanced perpendicular crystalline anisotropy of Pd/Co/Pd film upon annealing.

## CONCLUSION

We have demonstrated a simple method to synthesis CoPd alloy, by *in-situ* annealing of Pd(4nm)/Co(5nm)/Pd(4nm) trilayer film, which shows strong perpendicular magnetic anisotropy. In this method, any traditional conditions, like ultra thin Co layer or multilayer structured films, have not been adopted to achieve the desired PMA behavior. TEM-EDS together with the EXAFS analyses confirm the formation of high structural ordered CoPd alloy in the annealed film. Pd $L_3$-edge XANES analysis shows that there is an enhanced charge transfer from Co to Pd site in the annealed film in comparison with the as-grown film, and the charge transfer induces the magnetic moment in the film. The

enhanced Co 3*d* orbital/spin moment ratio plays major role in the perpendicular anisotropy observed in the annealed film.

**Acknowledgements**

The authors (BYW and WFP) are grateful to the Ministry of Science and Technology of Taiwan for financial support in this research under Grant No. NSC 102-2112-M-018-006-MY3 and 102-2112-M-032-007-MY3.

## REFERENCE


1. S. Mangin, D. Ravelosona, J. A. Katine, M. J. Carey, B.D. Terris, and E. E. Fullerton, Nature Mater., 2006, **5**, 210.
2. M. Jamali, K. Narayanapillai, X. Qiu, L. M. Loong, A. Manchon, and H. Yang, Phys. Rev. Lett., 2013, **111**, 246602.
3. A. D. Kent, B. Ozyilmaz, and E. del Barco, Appl. Phys. Lett., 2004, **84**, 3897.
4. J. Stöhr and H. C. Siegmann, *Magnetism: From fundamentals to Nanoscale Dynamics. (Springer; illustrated edition)* 12 Sep 2006.
5. K. Mizunuma, S. Ikeda, J.H. Park, H. Yamamoto, H. Gan, K. Miura, H. Hasegawa, J. Hayakawa, F. Matsukura and H. Ohno, Appl. Phys. Lett., 2009, **95**, 232516.
6. B. Carvello, C. Ducruet, B. Rodmacq, S. Auffret, E. Gautier, G. Gaudin, and B. Dieny, Appl. Phys. Lett., 2008, **92**, 102508.
7. G. Kim, Y. Sakuraba, M. Oogane, Y. Ando, and T. Miyazaki, Appl. Phys. Lett., 2008, **92**, 172502.
8. C. Boeglin, E. Beaurepaire, V. Halte, V. L. Flores, C. Stamm, N. Pontius, H. A. Dürr, and J. Y. Bigot, Nature, 2010, **465**, 458.
9. T. Das, P.D. Kulkarni, S.C. Purandare, H.C. Barshilia, S. Bhattacharyya, and P. Chowdhury, Sci. Rep., 2014, **4**, 5328.
10. S .Tsunashima, K. Nagase, K. Nakamura, and S. Uchiyama, IEEE Trans. Magn., 1989, **25**, 3761.
11. W. C. Lin, C. J. Tsai, B. Y. Wang, C. H. Kao, and W. F. Pong, Appl. Phys. Lett., 2013, **102**, 252404.
12. S. K. Kim, V. A. Chernov, J. B. Kortright, and Y. M. Koo, Appl. Phys. Lett.,

1997, **71**, 7.

13. J. Carrey, A. E. Berkowitz, Jr. W. F. Egelhoff, and D. J. Smith, Appl. Phys. Lett., 2003, **83**, 5259.
14. K. Yakushiji, T. Saruya, H. Kubota, A. Fukushima, T. Nagahama, S. Yuasa, and K. Ando, Appl. Phys. Lett., 2010, **97**, 232508.
15. P. F. Carcia, A. D. Meinhaldt, and A. Suna, Appl. Phys. Lett., 1985, **47**, 178.
16. F. J. A. den Broeder, H. C. Donkersloot, H. J. G. Draaisma, and W. J. M. de Jonge, J. Appl. Phys., 1987, **61**, 4317.
17. S. K. Kim and S. C. Shin, J. Appl. Phys., 2001, **89**, 3055.
18. S. K. Kim, J. W. Lee, J. R. Jeong, J. Kim, and S. C. Shin, Appl. Phys. Lett., 2001, **79**, 1652.
19. D. G. Stinson and S. C. Shin, J. Appl. Phys., 1990, **67**, 4459.
20. O. Yabuhara, M. Ohtake, K. Tobari, T. Nishiyama, F. Kirino, M. Futamoto, Thin Solid Films, 2011, **519**, 8359.
21. M. Gottwald, K. Lee, J. J. Kan, B. Ocker, J. Wrona, S. Tibus, J. Langer, S. H. Kang, and E. E. Fullerton, Appl. Phys. Lett., 2013, **102**, 052405.
22. S. K. Kim, Y. M. Koo, V. A. Chernov, J. B. Kortright, and S.C. Shin, Phys. Rev. B, 2000, **62**, 3025.
23. D. Weller, J. Stöhr, R. Nakajima, A. Carl, M. G. Samant, C. Chappert, R. Megy, P. Beauvillain, P. Veillet, and G.A. Held, Phys. Rev. Lett., 1995, **75**, 3752.
24. L. Néel, J. Phys. Radium, 1954, **15**, 225.
25. J. Miyawaki, D. Matsumura, A. Nojima, T. Yokoyama, and T. Ohta, Surf. Sci., 2007, **601**, 95.

26. T. K. Sham, Phys. Rev. B, 1985, **31**, 1903.
27. N. Nakajima, T. Koide, T. Shidara, H. Miyauchi, H. Fukutani, A. Fujimori, K. Iio, T. Katayama, M. Nývlt, and Y. Suzuki, Phys. Rev. Lett., 1998, **81**, 5229.
28. S. Barman, D.G. Kanhere and G.P. Das, J. Phys.: Condens. Matter., 2009, **21**, 396001.
29. C.T. Chen, Y.U. Idzerda, H.-J. Lin, N.V. Smith, G. Meigs, E. Chaban, G. H. Ho, E. Pellegrin and F. Sette, Phys. Rev. Lett., 1995, **75**, 152.
30. B. T. Thole, P. Carra, F. Sette, and G. van der Laan, Phys. Rev. Lett., 1992, **68**, 1943.
31. P. Carra, B. T. Thole, M. Altarelli, and X. D.Wang, Phys. Rev. Lett., 1993, **70**, 694.
32. D. M. S. Bagguley, W. A. Crossley, and J. Liesegang, Proc. Phys. Soc., 1967, **90,** 1047.
33. M.E. Gruner and A. Dannenberg, J. Magn. Magn. Mater., 2009, **321**, 861.
34. D. Weller, Y. Wu, J. Stöhr, M. G. Samant, B. D. Hermsmeier, and C. Chappert, Phys. Rev. B, 1994, **49**, 12888.
35. E. C. Stoner and E. P. Wohlfarth, Trans. R. Soc. A, 1948, **240**, 599.
36. P. Bruno, Phys. Rev. B, 1989, **39**, 865.
37. B. Y. Wang, J. Y. Hong, K. H. Ou Yang, Y. L. Chan, D. H. Wei, H. J. Lin, and M. T. Lin, Phys. Rev. Lett., 2013, **110**, 117203.Y. Matsuo, J. Phys. Soc. Jpn., 1972, **32**, 972.

**Figure captions**

**Fig. 1** In-plane and out-of-plane MOKE magnetic hysteresis loops of (a) as-grown and (b) annealed Pd/Co/Pd films. Insets show the corresponding cross-sectional TEM images and EDS scans across the interface of film. (c) and (d) are the in-plane and out-of-plane MOKE magnetic hysteresis loops of Pd-rich alloy and Co-rich alloys, respectively. Insets present the corresponding cross-sectional TEM images and the EDS analysis.

**Fig. 2** (a) Fourier-transformed Co *K*-edge EXAFS spectra of as-grown and annealed Pd/Co/Pd films and reference samples. Inset shows corresponding EXAFS $k^2\chi$ data, where $k$ is from 3.5 to 11 $Å^{-1}$. (b) Normalized Pd $L_3$-edge XANES spectra. Inset magnifies region of feature A.

**Fig. 3** The Co $L_{3,2}$-edge XAS spectra of the as-grown and annealed films and Co foil, Co-rich alloy and Pd-rich alloy with the sample magnetization parallel ($\mu_+$) and antiparallel ($\mu_-$) to direction of incident X-ray. Dashed lines represent integrated XAS spectra. Bottom panels show XMCD and integrated XMCD spectra.

**Tab. 1** Orbital ($m_{orb}$), spin ($m_{spin}$) moments and ratio of $m_{orb}/m_{spin}$ derived from the XMCD curves and sum-rules (in $\mu_B$ /atom unit).

| Sample | $m_{orb}$ | $m_{spin}$ | $m_{orb}/m_{spin}$ |
|---|---|---|---|
| *hcp*-Co[29] | 0.15 | 1.50 | 0.1 |
| Co foil | 0.20±0.05 | 1.50±0.05 | 0.13±0.05 |
| As-grown film | 0.37 ± 0.05 | 1.95 ± 0.05 | 0.19 ± 0.05 |
| Annealed film | 0.33 ± 0.05 | 1.48 ± 0.05 | 0.23 ± 0.05 |
| Co-rich alloy | 0.16 ± 0.05 | 1.37 ± 0.05 | 0.12 ± 0.05 |
| Pd-rich alloy | 0.10 ± 0.05 | 0.37 ± 0.05 | 0.27 ± 0.05 |

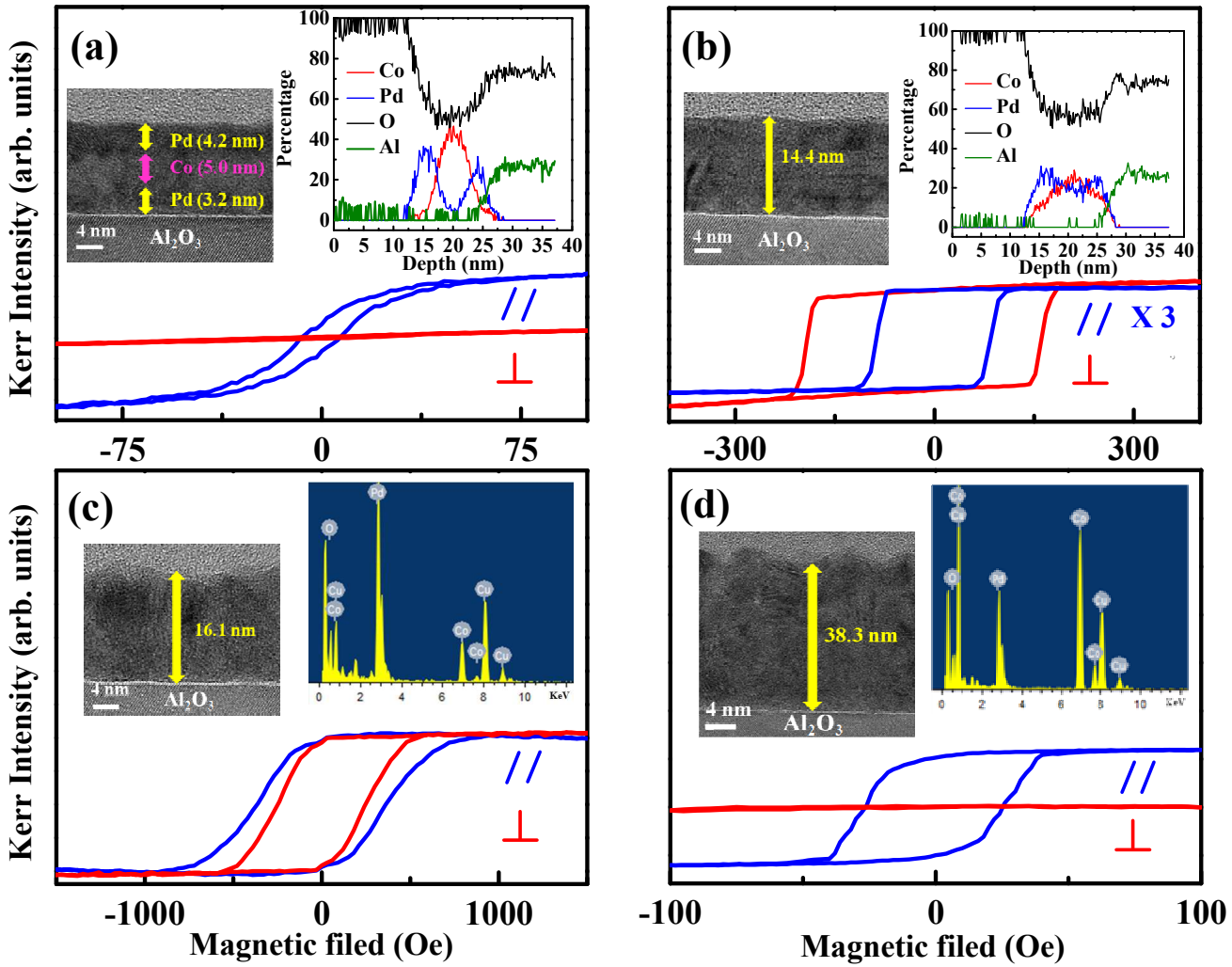


**Fig. 1**

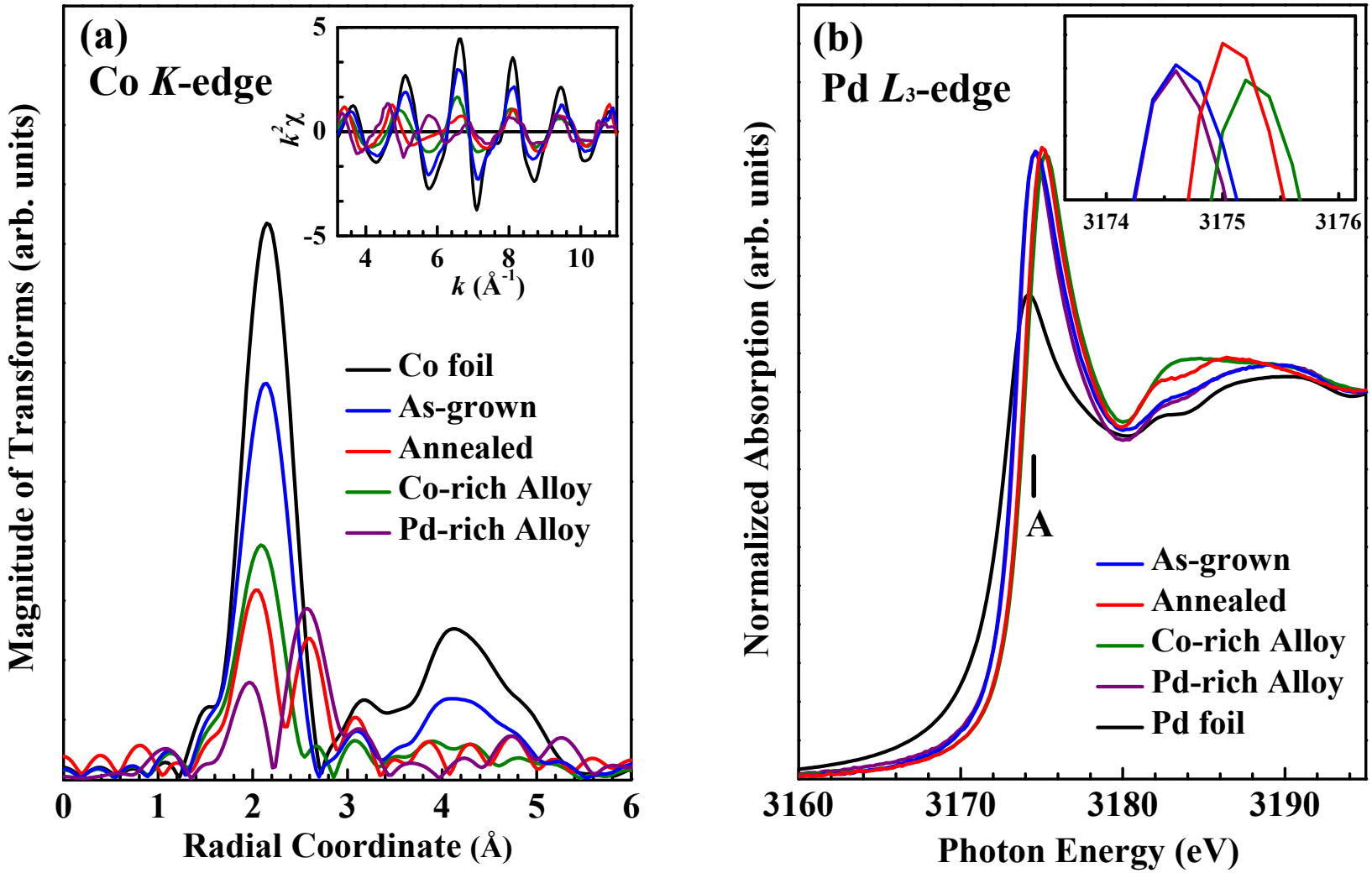


**Fig. 2**

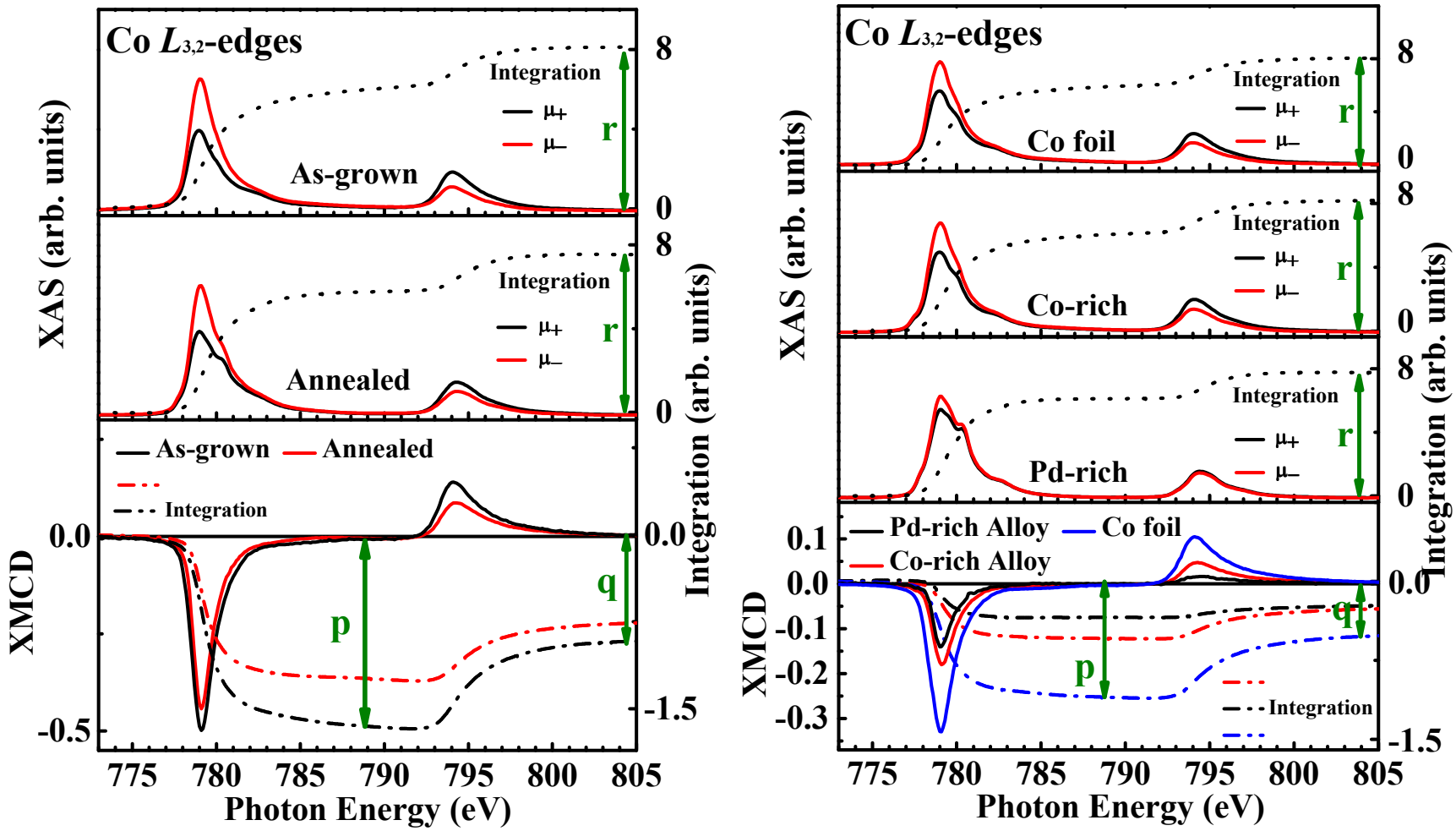


**Fig. 3**

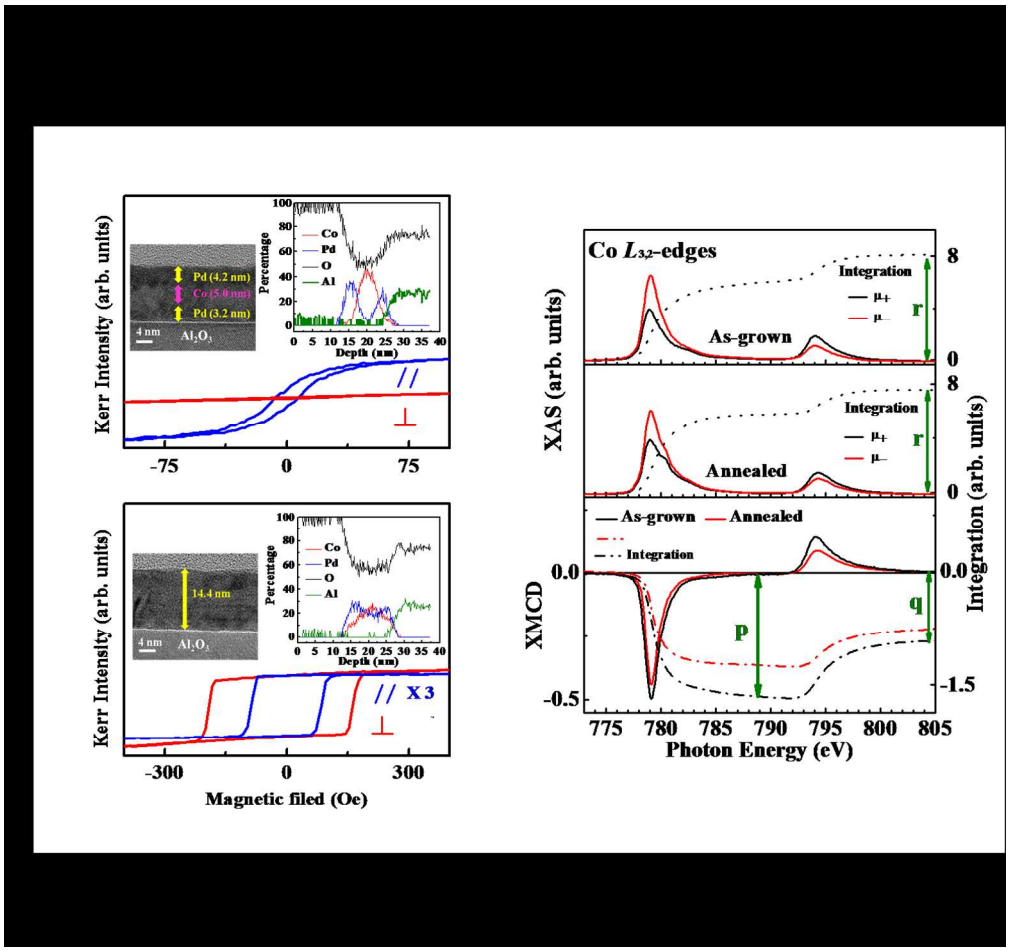


262x247mm (150 x 150 DPI)